ISSN 0960-1317

Journal of Micromechanics and Microengineering

Structures, devices and systems

Volume 22 Number 5 May 2012

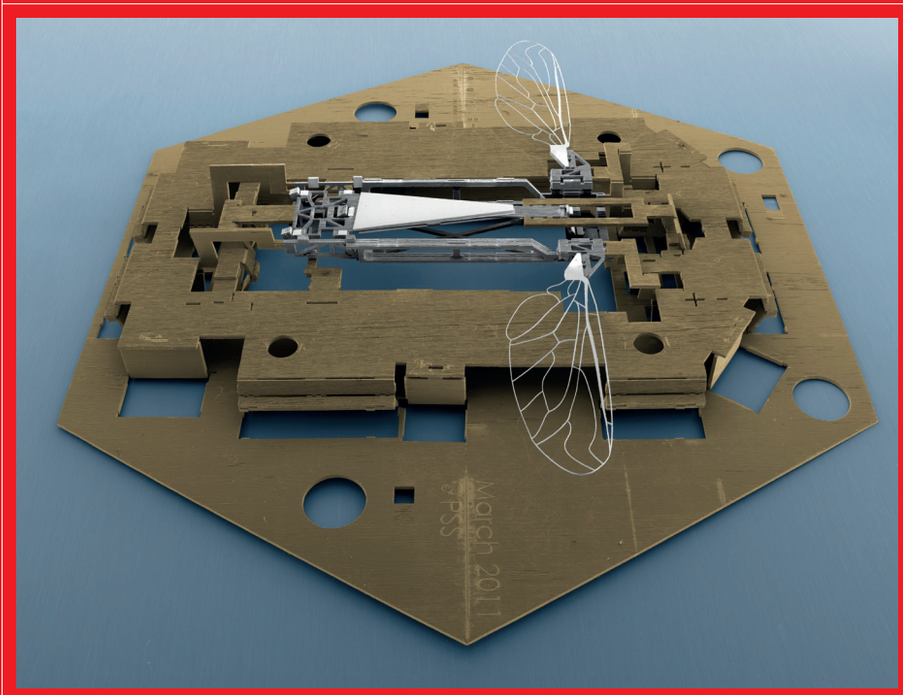

iopscience.org/jmm

IOP Publishing

Journal of Micromechanics and Microengineering

Vol 22, No 5 055001–057002

May 2012

J. Micromech. Microeng. **22** (2012) 055027 (6pp) doi:10.1088/0960-1317/22/5/055027

Monolithic fabrication of millimeter-scale machines

P S Sreetharan, J P Whitney, M D Strauss and R J Wood

Microrobotics Laboratory, Harvard University, 60 Oxford Street 407, Cambridge, MA 02138, USA

E-mail: pratheev@post.harvard.edu

Received 14 September 2011, in final form 13 February 2012
Published 23 April 2012
Online at stacks.iop.org/JMM/22/055027

Abstract
Silicon-based MEMS techniques dominate sub-millimeter scale manufacturing, while a myriad of conventional methods exist to produce larger machines measured in centimeters and beyond. So-called mesoscale devices, existing between these length scales, remain difficult to manufacture. We present a versatile fabrication process, loosely based on printed circuit board manufacturing techniques, for creating monolithic, topologically complex, three-dimensional machines in parallel at the millimeter to centimeter scales. The fabrication of a 90 mg flapping wing robotic insect demonstrates the sophistication attainable by these techniques, which are expected to support device manufacturing on an industrial scale.

Modern industry has developed a vast array of conventional techniques to produce machines at the familiar scales of centimeters to meters. Recent decades have also seen rapid development in the manufacture of microelectromechanical systems (MEMS), mostly based on silicon wafer processing techniques, with characteristic length scales of millimeters to nanometers. Numerous commercially successful MEMS devices exist, ranging from accelerometers to pressure sensors to displays, and more intricate devices such as electrostatic motors and miniaturized gas turbines have been created in the laboratory [1–4]. However, standard MEMS techniques are often inappropriate for producing larger machines with complex three-dimensional topology and varied constituent materials.

Many applications exist for devices in this mesoscale gap between conventional manufacturing and MEMS, with insect-inspired aerial robots being a notable motivating example. A flapping wing robotic insect requires advanced structural materials, actuators and topologies, creating challenges even for larger vehicles such as the 16 g Delfly II [5]. Lowering the mass target to 100 mg requires these features typical of conventionally manufactured devices at scales more closely associated with MEMS. Previous attempts to manufacture such devices have relied on highly skilled manual process steps [6–8]. Other projects seek to circumvent many manufacturing issues by modifying existing biological organisms to externally control behavior, e.g. in beetles and moths [9, 10]. Of course, such biological interfaces raise a different set of manufacturing hurdles, solved in one case by laminated manufacturing techniques [11]. Motivated by these challenges, we have developed a bulk-machined MEMS process, termed printed circuit MEMS (PC-MEMS), for creating mesoscale machines up to several centimeters in dimension.

In contrast with conventional MEMS techniques, which arose from integrated circuit fabrication technology, PC-MEMS draws inspiration from printed circuit board (PCB) manufacturing. PCB-inspired lamination has proved to be an effective underlying fabrication process for creating mesoscale MEMS devices such as RF switches [12]. Researchers have also created devices comparable to canonical flat MEMS devices, such as two-axis micromirrors and pressure sensors, at larger scales on laminated substrates [13, 14]. We have previously demonstrated folding three-dimensional assembly and self-assembly in laminated MEMS devices [15]. In this paper, we extend these techniques further to include pick-and-place components, 'locking' through wave soldering, scaffold-assisted assembly, increased material variety and integrated actuation, resulting in a manufacturing process capable of realizing actuated, fully three-dimensional millimeter-scale machines.

PC-MEMS machines can incorporate micron-scale mechanical features, piezoelectric actuators, integrated circuitry and a wide variety of materials in true three-dimensional topologies. The Harvard Monolithic Bee (Mobee), an exemplary PC-MEMS machine, is a 90 mg

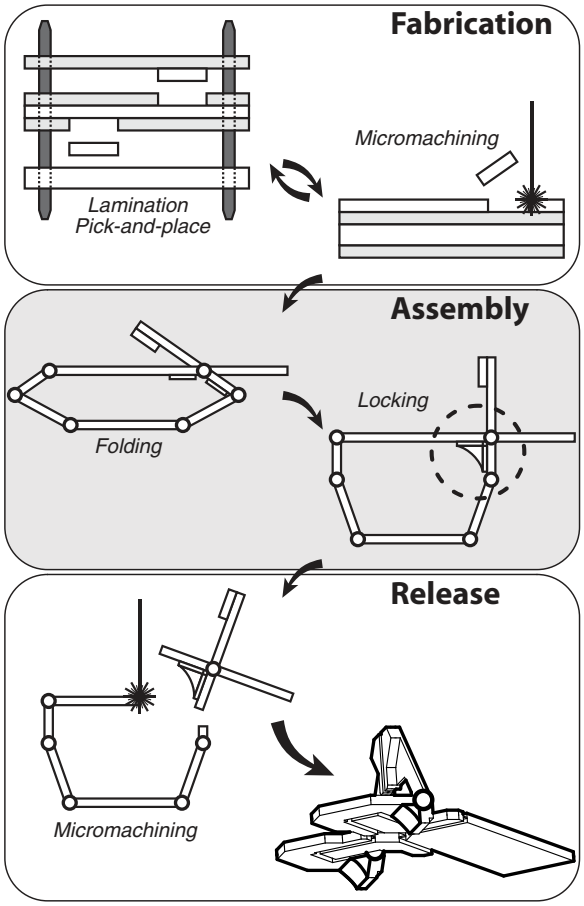

Figure 1. A schematic representation of the PC-MEMS process illustrates how the basic operations of micromachining, lamination, pick-and-place, folding and locking are arranged to manufacture PC-MEMS machines.

flapping-wing robotic insect with a 39 mm wingspan, a length of 18 mm and an out-of-plane height of 2.4 mm. Mobee emerges from the manufacturing process as an actuated, three-degree-of-freedom mesoscale machine, and serves as a useful demonstration of PC-MEMS capability.

1. PC-MEMS overview

The manufacturing process begins with material layers typically 1–250 μm thick and consists of four basic operations: additive lamination, subtractive micromachining, folding and locking (figure 1). A fifth operation, pick-and-place, allows inclusion of discrete components, such as sensors, actuators, integrated circuits and other MEMS or PC-MEMS devices, that do not topologically form full layers.

Figure 1 provides a schematic overview of the PC-MEMS process, which combines these basic operations with a special attention to controlling mechanical degrees of freedom. A sequence of micromachining and lamination steps fabricates flat multilayer laminates from individual material layers while ensuring that layers and sublaminates remain contiguous for effective alignment during lamination. Combining rigid and flexible materials enables flexure-based mechanical joints for articulated machine components and folding assembly, but these must remain constrained during fabrication. The final fabrication micromachining step releases all folding joints, which are coupled into a single-assembly degree of freedom, allowing three-dimensional machines to rise through precise 'pop-up' assembly. Subsequent locking bonds assembled machine components together, removing this degree of freedom and completing assembly. Lastly, micromachining releases all active degrees of freedom of the articulated machine. This methodology allows for parallel manufacture and straightforward assembly of complex three-dimensional machines.

A wide variety of materials including metals, plastics, ceramics and composites are compatible with PC-MEMS. Mobee uses five layers of 100 μm carbon fiber reinforced plastic (CFRP) for high-stiffness and low-mass structural components, one layer of 50 μm titanium alloy for finely featured, high-strength wings and two layers of 7.5 μm polyimide film for resilient flexure joints. Two 12.5 μm brass layers are involved in the locking process, while two discrete 127 μm lead zirconate titanate (PZT) piezoelectric ceramic plates form a bimorph actuator. Other devices have successfully used fiberglass composites, other metals such as steel, copper and aluminum and polymer films as thin as 1.5 μm. The ability to use a diverse array of bulk high-performance materials instead of only those that can be deposited, sputtered or plated is a key advantage of PC-MEMS. The full gamut of compatible materials depends on the chosen interlayer adhesive and has not yet been determined.

2. Fabrication

Fabrication begins by processing source material layers with a series of micromachining and lamination operations. Although many micromachining and lithographic techniques are applicable, we use a diode-pumped solid-state (DPSS) laser to micromachine individual source material layers, creating complex in-plane features as small as 10 μm. To realize out-of-plane mechanical features, a stack of micromachined structural layers are interleaved with similarly processed adhesive layers (Dupont Pyralux FR1500 12.5 μm sheet adhesive) for lamination. Inspired by PCB techniques, precision dowel pins provide persistent lateral alignment, while heat and pressure applied in a platen press cure the adhesive, creating a multilayer laminate [15]. The resulting laminates may themselves be treated as source material layers, undergoing further micromachining and inclusion as structural layers in subsequent lamination steps.

In contrast with highly serial existing MEMS processes, a large variety of devices can be constructed using only a single additive lamination step. Typically, layers are micromachined individually, laminated in parallel and the resulting laminate is micromachined again to prepare for folding assembly. We have demonstrated devices with ten structural layers laminated in parallel, though process limitations on layer count have not been determined. However, PCBs with 60 copper layers are commercially available, implying parallel lamination of more than one hundred structural layers[1].

[1] Sixty-layer PCBs can currently be purchased as standard products from Viasystems Group, Inc., of St Louis, MO, USA and from DDi Corp. of Anaheim, CA, USA, among others.

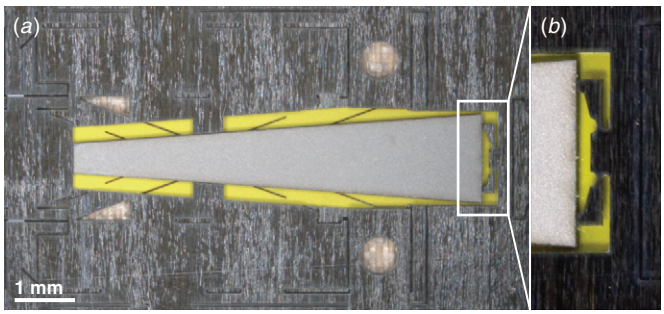

Figure 2. Pick-and-place. (*a*) Quasi-kinematic mating features and (*b*) in-plane flexure springs in a carbon fiber material layer align a discrete pick-and-place piezoelectric plate during lamination.

Sequential lamination steps can produce a different layer stack at different regions of a final laminate; shown schematically in figure 1, a raised region of one sublaminate can be inserted into a corresponding pocket in an adjacent sublaminate. In addition, sequential lamination eases the problem of clearing chips from internal layers after micromachining. By laminating sequentially, these internal layers can be exposed on the surface of an intermediate sublaminate for simplified micromachining. Mobee uses two sequential lamination steps to take advantage of both features.

The pick-and-place process extends the capabilities of lamination by allowing inclusion of discrete components and materials unsuited for pin alignment. Two structural layers of Mobee incorporate large pockets bordered by quasi-kinematic mating features and an in-plane flexure spring (figure 2). Discrete PZT plates inserted into these pockets are held in alignment during lamination, resulting in a high power density bimorph actuator [16]. PC-MEMS is compatible with more conventional pick-and-place techniques from the PCB industry, allowing populated circuit boards to be integrated into the mechanical structure (see [17]). This compatibility with PCB techniques parallels the CMOS compatibility of some silicon-based MEMS processes [18].

Incorporation of both flexible and rigid structural layers in a multilayer laminate allows creation of mechanical joints, components commonly used in conventional MEMS [19]. These flexure-based joints enable articulated PC-MEMS machines; figure 3(*a*) depicts a four-bar linkage with three flexure joints, used as a transmission to couple the power actuator with Mobee's wings. Figure 3(*d*) depicts a castellated 'folding joint,' a variant engineered to approximate an ideal revolute joint.

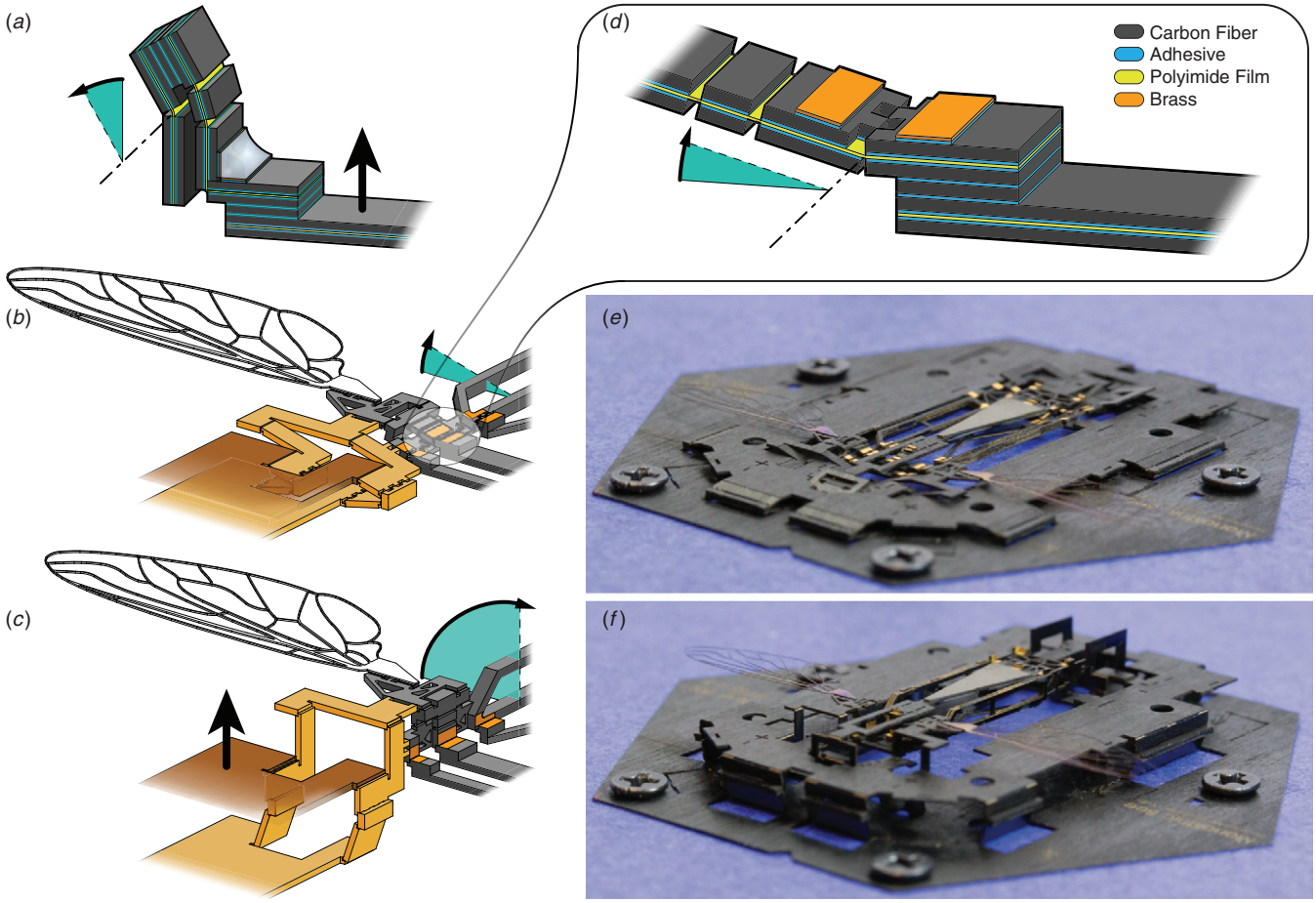

Figure 3. Topology and folding assembly of PC-MEMS devices. (*a*) A four-bar linkage containing three active joints used as a transmission, turning linear actuation into rotational wing motion. (*b*) Schematic representation of Mobee prior to and (*c*) after folding assembly, illustrating how the assembly scaffold (gold) drives assembly folds with a single degree of freedom. (*d*) Castellated folding joints enable precision folding. (*e*) Mobee prior to and (*f*) after folding assembly.

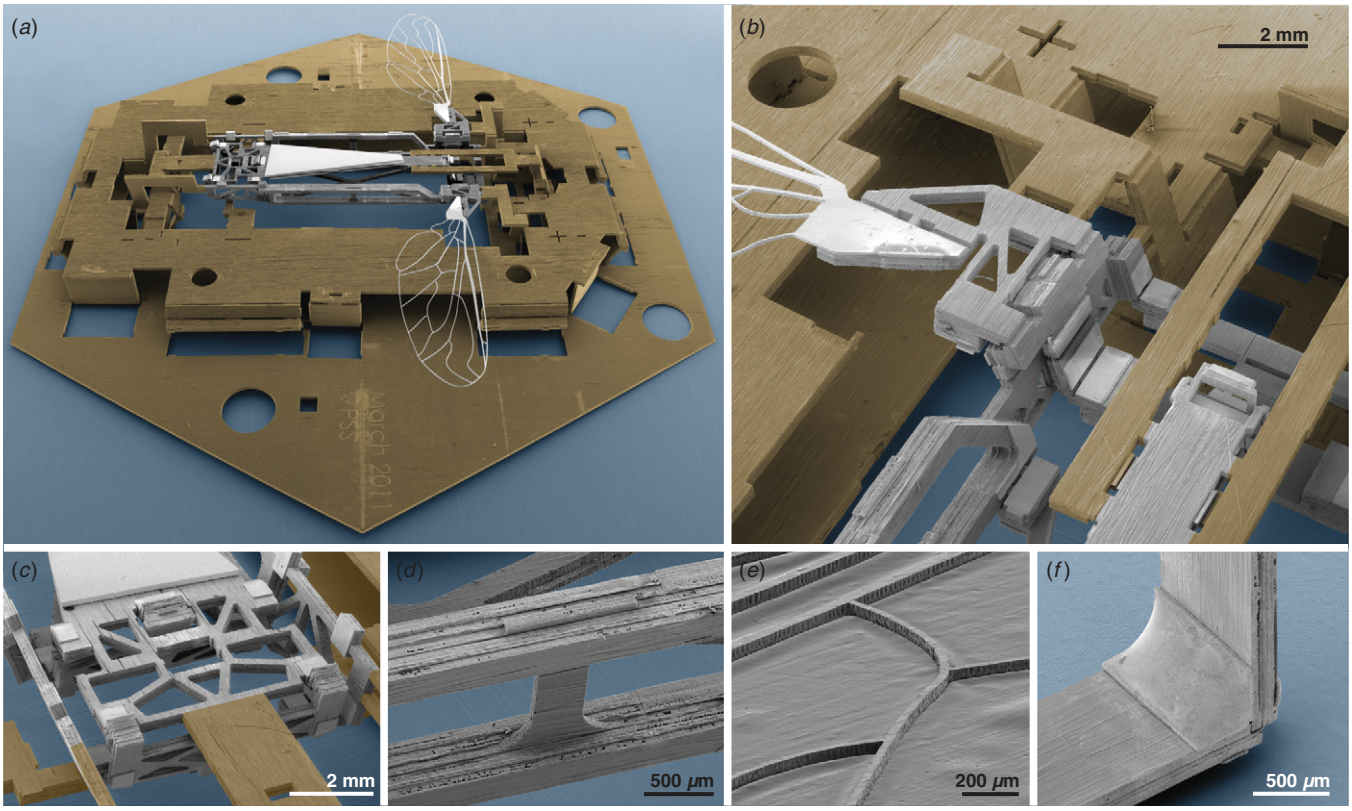

Figure 4. Scanning electron microscopy of PC-MEMS structures. All images are presented in false color, used to distinguish the background (blue), the assembly scaffold (gold) and the core machine (grayscale). (*a*) Mobee in its assembly scaffold after partial pop-up assembly. The hexagonal base has 25 mm edges. PC-MEMS devices can have three-dimensional, complex topology (*b*) and incorporate optimized mechanical structures such as (*c*) box trusses and (*d*) I-beams. (*e*) Titanium wing spars support a wing membrane. (*f*) A solder fillet locks a folding joint.

3. Assembly

After fabrication, the resulting multilayer mechanical structures have intricate in-plane features but remain flat with limited out-of-plane complexity. This restriction is widespread throughout MEMS; techniques to create truly three-dimensional structures include vastly increasing layer number (3D printing), assembly through origami folding and various self-assembly techniques [20–22]. We take an origami folding approach to assemble three-dimensional machines from flat multilayer laminates using a single 'pop-up' degree of freedom.

To minimize the impact of single-degree-of-freedom assembly on the device itself, all mechanical elements that drive assembly are collected into a co-fabricated assembly scaffold surrounding one or more unfolded machines. The assembly scaffold is a mechanical transmission constructed of rigid links and folding joints that couples all necessary assembly folds into a single degree of freedom, which is released by the final fabrication micromachining step. The use of an assembly scaffold eliminates vestigial assembly mechanisms in the final device and allows the creation of structures beyond those highly tailored for 'pop-up' assembly (see [15] for examples). Figures 3(*b*) and (*c*) illustrate the functioning of Mobee's assembly scaffold, highlighted in false color in figure 4(*a*).

Mobee's assembly scaffold is based on a Sarrus linkage: two parallel plates surround the device and can be separated in a single translational degree of freedom. Interior linkages, driven by the separating plates, create all necessary assembly trajectories. Although Mobee contains only 90° folds, altering the kinematics of these interior linkages can result in a wide range of folding angles in assembled devices. Figures 3(*b*) and (*c*) also demonstrate a more complex assembly trajectory: the wing translates along a circular arc without rotation. Mobee and its assembly scaffold together contain 137 folding joints linked into one assembly degree of freedom. Twelve additional joints that form a three-degree-of-freedom power transmission mechanism must remain mechanically constrained during assembly.

Separating the assembly scaffold plates with an external force initiates pop-up folding. Various mechanical parts interfere to form a joint stop, halting motion once folding is complete. Thus, assembly actuation need not be precise, and inclusion of material layers with stored elastic energy has already demonstrated self-assembly of a simple PC-MEMS device [15].

A wide variety of mechanical structures are available to folded PC-MEMS machines. The wing veins (figure 4(*e*)) are unsupported titanium beams, some of which have a $30\,\mu\text{m} \times 50\,\mu\text{m}$ cross section and extend over 7000 μm in length. A box truss (figure 4(*c*)) supports the base of Mobee's actuator and twin I-beams (figure 4(*d*)) form the airframe; these

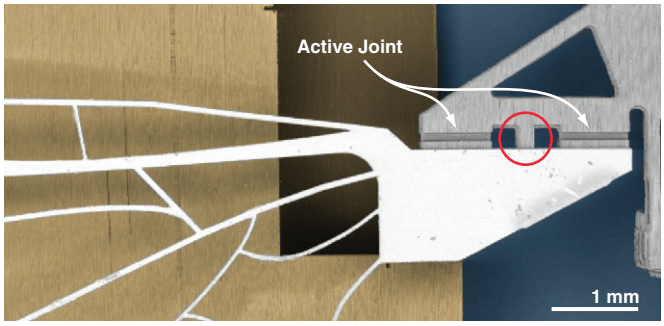

Figure 5. Mobee's wing is mounted in series with an active joint. The circled strut mechanically constrains this joint to ensure precision single degree of freedom assembly. This strut is one of several removed by micromachining during release to enable Mobee's three active degrees of freedom. The image is presented in false color.

optimized mechanical structures are usually available only in larger, conventionally manufactured machines.

Folding accuracy fundamentally depends on the determinism of folding joint motion and the stiffness of mechanical elements in resisting torques arising from flexure-based joints. Figure 3(*d*) illustrates a 'folding joint,' a flexure joint designed to minimize axis drift. Reducing flexure joint stiffness combats the deformation of mechanical elements, and joint stops combined with slight overactuation of the assembly scaffold can also aid folding accuracy. Photogrammetric measurement of the box truss of a completed Mobee revealed the assembly fold angle to be 3.7° below its intended value of 90°.

Once the mechanism is folded, removing the assembly degree of freedom through locking completes machine assembly. Various mechanical latching mechanisms have been demonstrated in MEMS folding, but again taking inspiration from PCB manufacturing, we have chosen a wave soldering approach [22]. Mobee contains two brass layers forming 52 solder pads. After folding, these pads align at 24 bond points, each consisting of two or three pads meeting at right angles. The entire device is submerged in flux (Superior No. 30) and then in a molten tin–lead eutectic solder. The solder bonds selectively to the brass pads, creating fillets at all bond points in parallel (figure 4(*f*)). These solder fillets eliminate the assembly degree of freedom, completing machine assembly.

4. Release

A final micromachining step releases the machine, concluding a typical PC-MEMS process. Although a PC-MEMS machine can have many active degrees of freedom, the assembly scaffold along with supplemental internal mechanical connections eliminate these degrees of freedom during fabrication and assembly. Figure 5 depicts an active degree of freedom in the Mobee's transmission mechanism constrained by an internal strut. During release, micromachining severs all connections between the assembly scaffold and the machine and removes all internal struts that constrain active degrees of freedom. Mobee has three active degrees of freedom, and the removal of three internal struts allows it to operate as a fully functional micromachine (figure 6).

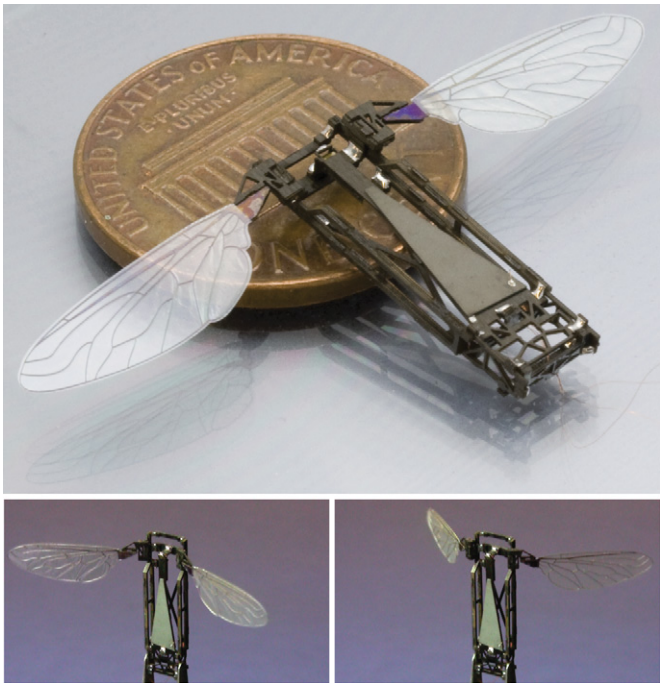

Figure 6. A completed Mobee (top) on a US penny and two video frames (bottom) demonstrating flapping motion.

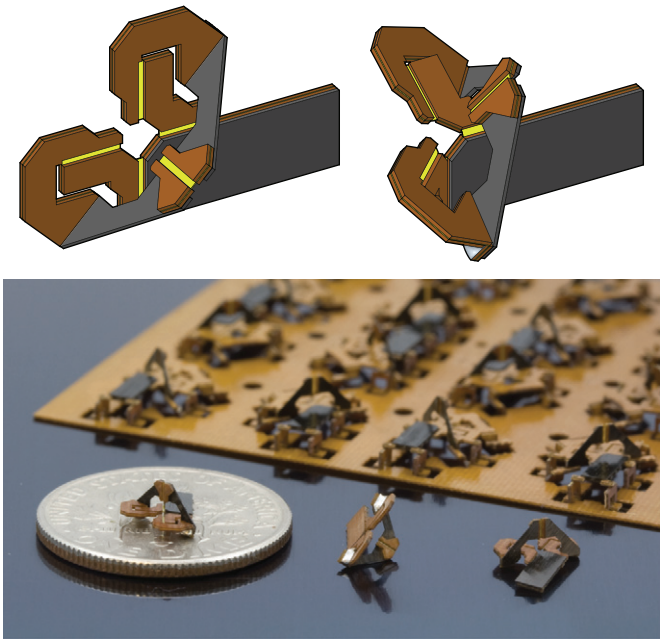

Figure 7. Top: a schematic representation of a spherical five-bar linkage in neutral and bent configurations. Bottom: three completed spherical five-bar linkages in front of a larger panel used to mass-produce them. A US dime provides scale.

5. Discussion and conclusion

The PC-MEMS process bridges the mesoscale gap in manufacturing techniques, providing a versatile framework to produce machines at the millimeter to centimeter scales. PC-MEMS devices are produced monolithically in parallel, an advantage shared by many MEMS processes. This feature promotes mass production, which can be seen in figure 7

depicting the parallel manufacture of 16 PC-MEMS spherical five-bar linkages. In addition, the highly parallel nature of lamination allows shorter lead times; Mobee has been manufactured within 24 h using academic research facilities. Other features such as material variety and topological complexity bring elements of conventional manufacturing to a MEMS process.

Ongoing research continues to improve PC-MEMS techniques. Assembly accuracy needs both optimization and full characterization. Wave solder locking imposes thermal requirements and selectivity constraints, and requires careful attention to solder flow around complex topologies, limitations that motivate the investigation of solder masks, solder reflow and solderless locking in PC-MEMS. The need for physical chip removal and the lack of design software impede the development of devices with extremely high layer counts. Finally, PC-MEMS compatibility with PCB manufacturing provides an avenue to integrate electronics and circuitry directly into the mechanical structure of millimeter-scale machines, and demonstration of this capability is a research priority.

Although developed to enable the production of millimeter-scale robotic systems, we expect the underlying manufacturing process to have a wide impact beyond the field of robotics. The potential for these larger, more versatile MEMS devices may extend into a diverse collection of fields such as medical robotics, power electronics, sensing, spectroscopy, metamaterials and others. Demand for these mesoscale machines from scientists and engineers in these fields will inspire future expansion and refinement of the PC-MEMS process.

Acknowledgments

The authors thank Dr James Weaver for providing SEM imagery. This work was partially supported by the Army Research Laboratory (award number W911NF-08-2-0004), the National Science Foundation (award number CCF-0926148) and the Wyss Institute for Biologically Inspired Engineering. Any opinions, findings and conclusions or recommendations expressed in this material are those of the authors and do not necessarily reflect the views of the National Science Foundation.

References

[1] Petersen K E 1982 Silicon as a mechanical material *Proc. IEEE* **70** 420–57

[2] Judy J W 2001 Microelectromechanical systems (MEMS): fabrication, design and applications *Smart Mater. Struct.* **10** 1115

[3] Tang W C, Nguyen T C H, Judy M W and Howe R T 1990 Electrostatic-comb drive of lateral polysilicon resonators *Sensors Actuators* A **21** 328–31

[4] Fréchette L G, Jacobson S A, Breuer K S, Ehrich F F, Ghodssi R, Khanna R, Wong C W, Zhang X, Schmidt M A and Epstein A H 2005 High-speed microfabricated silicon turbomachinery and fluid film bearings *J. Microelectromech. Syst.* **14** 141–52

[5] Groen M, Bruggeman B, Remes B, Ruijsink R, van Oudheusden B W and Bijl H 2010 Improving flight performance of the flapping wing MAV DelFly II *Int. Micro Air Vehicle Conf. and Competition (IMAV 2010) (Braunschweig, Germany)* http://www.delfly.nl/?site=Publications&menu=&lang=nl

[6] Wood R J, Avadhanula S, Sahai R, Steltz E and Fearing R S 2008 Microrobot design using fiber reinforced composites *J. Mech. Des.* **130** 052304

[7] Fearing R S, Chiang K H, Dickinson M H, Pick D L, Sitti M and Yan J 2001 Wing transmission for a micromechanical flying insect *J. Micromechatronics* **1** 221–37

[8] Wood R J 2008 The first takeoff of a biologically inspired at-scale robotic insect *IEEE Trans. Robot.* **24** 341–7

[9] Sato H and Maharbiz M M 2010 Recent developments in the remote radio control of insect flight *Front. Neurosci.* **4** 199

[10] Daly D C, Mercier P P, Bhardwaj M, Stone A L, Aldworth Z N, Daniel T L, Voldman J, Hildebrand J G and Chandrakasan A P 2010 A pulsed UWB receiver SoC for insect motion control *IEEE J. Solid-State Circuits* **45** 153–66

[11] Bozkurt A and Lal A 2011 Low-cost flexible printed circuit technology based microelectrode array for extracellular stimulation of the invertebrate locomotory system *Sensors Actuators* A **169** 89–97

[12] Ramadoss R, Lee S, Lee Y C, Bright V M and Gupta K C 2003 Fabrication, assembly and testing of RF MEMS capacitive switches using flexible printed circuit technology *IEEE Trans. Adv. Packag.* **26** 248–54

[13] Bachman M and Li G-P 2011 MEMS in laminates *IEEE 61st Electronic Components and Technology Conf. (ECTC) (May 31–June 3 2001)* pp 262–7

[14] Palasagaram J N and Ramadoss R 2006 MEMS-capacitive pressure sensor fabricated using printed-circuit-processing techniques *IEEE Sensors J.* **6** 1374–5

[15] Whitney J P, Sreetharan P S, Ma K Y and Wood R J 2011 Pop-up book MEMS *J. Micromech. Microeng.* **21** 115021

[16] Wood R J, Steltz E and Fearing R S 2005 Optimal energy density piezoelectric bending actuators *Sensors Actuators* A **119** 476–88

[17] Chang S P and Allen M G 2004 Demonstration for integrating capacitive pressure sensors with read-out circuitry on stainless steel substrate *Sensors Actuators* A **116** 195–204

[18] Bustillo J M, Howe R T and Muller R S 1998 Surface micromachining for microelectromechanical systems *Proc. IEEE* **86** 1552–74

[19] Pister K S J and Judy M W *et al* 1992 Microfabricated hinges *Sensors Actuators* A **33** 249–56

[20] Cohen A, Zhang G, Tseng F-G, Frodis U, Mansfeld F and Will P 1999 EFAB: rapid, low-cost desktop micromachining of high aspect ratio true 3-D MEMS *12th IEEE Int. Conf. Micro Electro Mech. Syst. (17–21 January 1999)* pp 244–51

[21] Hui E E, Howe R T and Rodgers M S 2000 Single-step assembly of complex 3-D microstructures *13th IEEE Int. Conf. Micro Electro Mech. Syst. (23–27 January 2000)* (IEEE) pp 602–7

[22] Syms R R A, Yeatman E M, Bright V M and Whitesides G M 2003 Surface tension-powered self-assembly of microstructures—the state-of-the-art *J. Microelectromech. Syst.* **12** 387–417